

Rescattering effects in coherent pion photoproduction on the deuteron in the Δ resonance region*

P. Wilhelm and H. Arenhövel

Institut für Kernphysik, Universität Mainz, D-55099 Mainz, Germany

Abstract

Within a dynamical model, rescattering effects are studied in coherent pion photoproduction on the deuteron in the $\Delta(1232)$ resonance region. The model consists of a system of coupled equations for the $N\Delta$, $NN\pi$ and NN channels. Pion rescattering leads in general to a significant reduction of total and differential cross sections resulting in a better description of experimental data. Only a few polarization observables are sensitive to rescattering effects. In particular T_{20} allows an analysis of the reaction mechanism for specific kinematics. The question how rescattering affects the sensitivity to the E2 excitation of the Δ resonance is also studied.

PACS numbers: 13.60.Le, 21.45.+v, 25.20.Lj

Typeset using REVTeX

*Supported by the Deutsche Forschungsgemeinschaft (SFB 201)

I. INTRODUCTION

Recently, we have studied coherent pion photoproduction on the deuteron neglecting rescattering effects in [1], henceforth referred to as I. Our justification for this work was to study systematically the details of the elementary production amplitude on the one hand, and on the other, to investigate the influence of genuine two-nucleon mechanisms which had not been considered before. However, the comparison of theoretical predictions and experimental data in I as well as in previous studies (see e.g. [2]) gave clear indication of important rescattering effects.

In most of former work, see e.g. [3–5], the rescattering of the pion was taken into account only perturbatively. For a recent study including single- and double-scattering diagrams, we refer to the work of Garcilazo and Moya de Guerra [6]. It is known that neutral pion production for photon energies just above threshold up to, say 450 MeV, is dominated by intermediate Δ resonance excitation via an electromagnetic M1 transition and subsequent p wave pion emission. However, it seems rather questionable whether a strong interacting system like the $N\Delta$ system in a relative 5S_2 partial wave with vanishing angular momentum barrier can be treated perturbatively at all. Thus a full dynamical treatment of at least the $N\Delta$ system appears mandatory, and it is the aim of this paper to develop such a description.

Only recently, different non-perturbative treatments of pion rescattering in $\gamma d \rightarrow \pi^0 d$ became available which can be applied in the Δ region. Blaazer, Bakker and Boersma [7] used the Faddeev equations for the πNN system. One of their main conclusions was that only the rescattering on the single-nucleon level is significant whereas genuine three-body effects turn out to be fairly unimportant in the Δ region. In a very recent work, Kamalov, Tiator and Bennhold applied the KMT multiple scattering approach [8] to coherent pion photoproduction [9] as well as to elastic pion scattering on the deuteron [10]. A characteristic feature of their approach is that it neglects the contributions from the coupling with the break-up channels. We will discuss below in some detail the shortcomings of this assumption. A dynamical treatment of the Δ , conceptually similar to the present work, has been used

by Peña et al. [11]. However, the main point of their paper was not the $\gamma d \rightarrow \pi^0 d$ reaction itself, and therefore, the presentation of their results is very brief. Moreover, the treatment of the nonresonant amplitudes and the input on the electromagnetic side is not clear.

Despite all these efforts, no common conclusions as to the importance of rescattering effects is reached. In fact, the various approaches even disagree qualitatively. For example at 300 MeV photon energy, the rescattering amplitudes of Ref. [9] within the KMT approach reduce the cross section. Their influence grows with increasing pion angle up to a reduction by a factor three at 180 deg. Also within the Faddeev ansatz of Ref. [7], the cross section is reduced in the forward direction by rescattering but at backward angles it is slightly increased. Unfortunately, the results shown in Ref. [11] do not allow to separate the rescattering influence. Thus the role of pion rescattering in $\gamma d \rightarrow \pi^0 d$ is by no means settled and requires further investigation.

This paper is organized as follows. In Section II we present our dynamical model for the $N\Delta$ system. As a test of the model, cross sections for pion deuteron elastic scattering are shown in Section III. The rescattering contributions which follow from the application of the model to coherent pion photoproduction on the deuteron are given in Section IV. The rescattering of charged pions which have not been produced by an initial electromagnetic excitation of the Δ is added in an approximate way. Our results for $\gamma d \rightarrow \pi^0 d$ are presented in Section V. Some emphasis is put on the role of charge exchange in the rescattering process. In our study of polarization observables we focus on the tensor target asymmetry T_{20} which may help to disentangle different reaction mechanisms. Finally, we study the sensitivity of the vector target asymmetry T_{11} to the E2 excitation of the Δ resonance.

II. DYNAMICAL MODEL FOR THE $N\Delta$ SYSTEM

The theoretical concept of our model with respect to the hadronic part is mainly based on the developments of Sauer and collaborators [12,13] and is similar to the treatment of Lee et al. in Ref. [14–17]. The model includes explicit pion, nucleon and delta degrees of

freedom. Hence its configuration space \mathcal{H} is built up from NN-, N Δ - and π NN-sectors

$$\mathcal{H} = \mathcal{H}_{NN} \oplus \mathcal{H}_N \oplus \mathcal{H}_{\pi NN}. \quad (1)$$

Corresponding projectors are denoted as P_N , P_Δ and Q , and we use for any operator Ω the obvious notation $\Omega_{N\Delta} = P_N \Omega P_\Delta$, $\Omega_{\Delta Q} = P_\Delta \Omega Q$, etc. The hamiltonian, $H = H_0 + V$, contains the kinetic energy H_0 and an interaction V which can be split up according to the various sectors

$$V = \sum_{X,Y=N,\Delta,Q} V_{XY}. \quad (2)$$

In the spirit of this model, we assume $V_{NQ} = V_{QN} = 0$, i.e., there is no explicit π NN-vertex leading to a direct coupling between NN- and π NN-sector. The creation or annihilation of a pion is exclusively due to the π N Δ vertex v_Δ already introduced in (I,19). It defines $V_{\Delta Q} = v_\Delta(1) + v_\Delta(2)$ and $V_{Q\Delta} = v_\Delta^\dagger(1) + v_\Delta^\dagger(2)$. As a further approximation, we switch off the diagonal interaction inside the π NN-sector completely, i.e., $V_{QQ} = 0$. With the latter simplification, the problem is essentially reduced to an effective two-body one. This holds irrespective of the specific form assumed for the remaining interactions $V_{\Delta N}$, $V_{N\Delta}$, V_{NN} , and $V_{\Delta\Delta}$. All dynamics is contained in a transition amplitude T which obeys a coupled integral equation of the Lippmann-Schwinger type

$$T_{NN}(W^+) = V_{NN} + V_{NN}G_N(W^+)T_{NN}(W^+) + V_{N\Delta}G_\Delta(W^+)T_{\Delta N}(W^+), \quad (3)$$

$$T_{\Delta N}(W^+) = V_{\Delta N} + V_{\Delta N}G_N(W^+)T_{NN}(W^+) + V_{\Delta\Delta}^{eff}(W^+)G_\Delta(W^+)T_{\Delta N}(W^+),$$

$$T_{N\Delta}(W^+) = V_{N\Delta} + V_{NN}G_N(W^+)T_{N\Delta}(W^+) + V_{N\Delta}(W^+)G_\Delta(W^+)T_{\Delta\Delta}(W^+),$$

$$T_{\Delta\Delta}(W^+) = V_{\Delta\Delta}^{eff}(W^+) + V_{\Delta N}G_N(W^+)T_{N\Delta}(W^+) + V_{\Delta\Delta}^{eff}(W^+)G_\Delta(W^+)T_{\Delta\Delta}(W^+),$$

where W is the invariant mass of the system. In (3), G_Δ denotes the dressed propagator of the noninteracting N Δ states, already introduced in (I,41-42), and

$$G_N(W^+) = [W + i\epsilon - h_N(1) - h_N(2)]^{-1} \quad (4)$$

is the free propagator in the NN-sector with the free nucleon energy $h_N = M_N + \vec{p}^2/(2M_N)$.

For the present application, the most relevant part of the driving term in (3) is $V_{\Delta\Delta}^{eff}(z)$ which describes the N- Δ interaction. It contains a retarded (ret) and thus energy-dependent pion exchange $V_{\Delta\Delta}^{ret}(z)$ and a static part which is just given by $V_{\Delta\Delta}$,

$$V_{\Delta\Delta}^{eff}(z) = V_{\Delta\Delta}^{ret}(z) + V_{\Delta\Delta}. \quad (5)$$

The first one follows from the iteration of the $\pi N\Delta$ vertex leading to

$$V_{\Delta\Delta}^{ret}(z) = \left(V_{\Delta Q} \frac{1}{z - H_0} V_{Q\Delta} \right)_{[2]}, \quad (6)$$

where the subscript [2] indicates the restriction to the two-body part of the operator. Besides the propagator G_Δ , this effective potential $V_{\Delta\Delta}^{ret}(z)$ contains implicitly a coupling to the three-body sector as required by three-body unitarity. Furthermore, the above mentioned neglect of an interaction in the πNN space ($V_{QQ} = 0$) leads to a partial violation of two-body unitarity since the coupling to intermediate πd states is not included.

In detail we obtain for (6)

$$V_{\Delta\Delta}^{ret}(z) = \vec{\tau}_{\Delta N}(1) \cdot \vec{\tau}_{N\Delta}(2) \int \frac{d^3q}{(2\pi)^3 2\omega_{\vec{q}}} e^{i\vec{q}\cdot\vec{r}} \frac{\vec{\sigma}_{\Delta N}(1) \cdot \vec{q} \vec{\sigma}_{N\Delta}(2) \cdot \vec{q}}{z - \omega_{\vec{q}} - h_N(1) - h_N(2)} \frac{F_\Delta^2(\vec{q}^2)}{m_\pi^2} + (1 \leftrightarrow 2), \quad (7)$$

where $\omega_{\vec{q}} = (m_\pi^2 + \vec{q}^2)^{1/2}$. The $\pi N\Delta$ form factor F_Δ is given in (I,22) and the normalization of the spin (isospin) operators $\vec{\sigma}_{N\Delta}$ ($\vec{\tau}_{N\Delta}$) in (I,21). In order to arrive at (7) we have dropped the transformation (I,20), i.e., we have replaced $\vec{q}_{\pi N}$ by \vec{q} in the $\pi N\Delta$ vertex (I,19).

For the static potential $V_{\Delta\Delta}$, we consider only pion exchange associated with intermediate $\pi\Delta\Delta$ states and neglect heavier meson contributions. Thus $V_{\Delta\Delta}$ follows from (7) by setting $z - h_N(1) - h_N(2) = 0$ in the denominator. In addition, V contains a $NN \leftrightarrow N\Delta$ transition potential $V_{N\Delta} = V_{\Delta N}^\dagger$ which is given in Appendix B and a diagonal NN interaction V_{NN} which is based on the OBEPR parametrization of the Bonn potential [18]. In view of the fact that the coupling to intermediate two-nucleon states turns out to be very small for coherent pion photoproduction we give no details on the construction of V_{NN} here and refer to [19] for the specification of this part of the potential where the model was applied to two-body deuteron photodisintegration.

For the explicit calculation we have solved Eq. (3) numerically in momentum space. Some details are given in Appendix A.

III. PION DEUTERON ELASTIC SCATTERING AS A TEST OF THE MODEL

Before we apply the hadronic interaction model to coherent pion photoproduction, we will first consider elastic pion deuteron scattering as a test case. Within our model, the amplitude for this process consists of a direct (Δ) and a rescattering (R) term, $T_{\pi d} = T_{\pi d}^{(\Delta)} + T_{\pi d}^{(R)}$, corresponding to the diagrams in Fig. 1 with

$$T_{\pi d}^{(\Delta)}(W_{\pi d}^+) = V_{Q\Delta} G_{\Delta}(W_{\pi d}^+) V_{\Delta Q}, \quad (8)$$

$$T_{\pi d}^{(R)}(W_{\pi d}^+) = V_{Q\Delta} G_{\Delta}(W_{\pi d}^+) T_{\Delta\Delta}(W_{\pi d}^+) G_{\Delta}(W_{\pi d}^+) V_{\Delta Q}, \quad (9)$$

where $W_{\pi d}$ is the invariant mass of the process. We show in Fig. 2 the resulting differential cross sections for various pion energies. Apparently, the rescattering contribution, which reduces the cross section up to a factor two at backward angles, leads to a considerably better description of the data in the resonance region ($W_{\pi d} = M_N + M_{\Delta}$ corresponds to the kinetic pion laboratory energy $T_{lab}^{\pi} \approx 180$ MeV) although at backward angles some overestimation remains. From this we conclude that the model presents a reasonable starting point to study pion rescattering effects in $\gamma d \rightarrow \pi^0 d$.

IV. APPLICATION TO COHERENT PION PHOTOPRODUCTION

Now we will turn to coherent pion photoproduction on the deuteron in order to study the rescattering effects generated by our hadronic interaction model. We show in Fig. 3 explicitly all diagrams of the process included in this work which go beyond the ones considered in I. The latter are summarized by $T_{\gamma\pi^0}^{IA}$ and shown in Fig. 4 separately for completeness. They include the impulse approximation diagrams, namely the direct Δ excitation $\Delta[1]$, the direct and crossed nucleon pole terms NP[1] and NC[1], respectively, and the disconnected direct and crossed two-nucleon processes, NP[2] and NC[2], respectively. Formally, the graphs NP

and NC follow from the π NN vertex v_N^\dagger defined in (I,9). This explicit vertex, which defines $V_{QN} = v_N^\dagger(1) + v_N^\dagger(2)$ and $V_{NQ} = v_N(1) + v_N(2)$, is however treated in first order only.

The common feature of the diagrams in Fig. 4 is that the hadronic intermediate state, either Δ N, NN or π NN, propagates freely. In principle each diagram will be accompanied by a corresponding one, where the intermediate state is subject to the hadronic interaction. Furthermore, the interaction will allow couplings between different intermediate states. In this work, however, we will restrict the interaction to the intermediate N Δ state resulting in the rescattering amplitude R $\Delta\Delta$ and to the NN-N Δ coupling R Δ N in Fig. 3. The contribution of R $\Delta\Delta$ to the T -matrix reads in the notation of I

$$T_{m'\lambda m}^{R\Delta\Delta}(\vec{q}, \vec{k}) = -\vec{\epsilon}_\lambda \cdot \langle \vec{q}, m' | V_{Q\Delta} G_\Delta(W_{\gamma d}^+) T_{\Delta\Delta}(W_{\gamma d}^+) \vec{J}_{\Delta N[1]}(E_\Delta, \vec{k}) | m \rangle, \quad (10)$$

where the one-body Δ excitation current $\vec{J}_{\Delta N[1]}$ has been defined in (I,25-26) and (I,42-43). In R Δ N the photon is first absorbed by the one-nucleon current $\vec{J}_{NN[1]}$ of (I,10) and (I,50) with subsequent NN-N Δ transition via $T_{\Delta N}$. Its T -matrix contribution is given by

$$T_{m'\lambda m}^{R\Delta N}(\vec{q}, \vec{k}) = -\vec{\epsilon}_\lambda \cdot \langle \vec{q}, m' | V_{Q\Delta} G_\Delta(W_{\gamma d}^+) T_{\Delta N}(W_{\gamma d}^+) \vec{J}_{NN[1]}(\vec{k}) | m \rangle. \quad (11)$$

However, it turns out that R $\Delta\Delta$ is by far the dominant process. Therefore, we will not separate the two contributions in the presentation of our results. In addition to these rescattering processes, we consider also meson exchange current contributions.

A. Meson exchange currents

So far we have mainly focused on the rescattering of pions which have been initially produced via the excitation of the Δ resonance. For charged pion production, there are, however, also strong background contributions, namely, the seagull and the pion pole graph. The reabsorption on the second nucleon of a pion which has been produced by one of these mechanisms contributes to the π -meson exchange current (π -MEC). Strictly speaking, a reabsorption involving an excitation of a Δ (Figs. 5a, b) corresponds to a subsequent

rescattering in the $P_{33}(\pi N)$ channel whereas a reabsorption without Δ excitation (Figs. 5d, e) contributes to rescattering in the $P_{11}(\pi N)$ channel. Considering the different time-orderings contained in the diagrams of Fig. 5, it is clear, that only the diagrams with forward propagating pions can be interpreted as a pion rescattering process. The graph of Fig. 5c appears through minimal coupling and is required by gauge invariance. In addition, we also include the ρ -MEC. Altogether, the two-body current $\vec{j}_{[2]}$ is given by

$$\vec{j}_{[2]} = \vec{j}_{[2]\Delta N}^{\pi} + \vec{j}_{[2]NN}^{\pi} + \vec{j}_{[2]NN}^{\rho}. \quad (12)$$

All terms in (12) are evaluated using the static approximation for the intermediate baryon propagation. Explicit expressions are given in Appendix B. They generate the following amplitudes including rescattering with X standing for Δ or N

$$T_{m'\lambda m}^{X[2]}(\vec{q}, \vec{k}) = -\vec{\epsilon}_{\lambda} \cdot \langle \vec{q}, m' | V_{QX} G_X(W_{\gamma d}^+) \vec{j}_{[2]XN}(\vec{k}) | m \rangle, \quad (13)$$

$$T_{m'\lambda m}^{RX[2]}(\vec{q}, \vec{k}) = -\vec{\epsilon}_{\lambda} \cdot \langle \vec{q}, m' | V_{Q\Delta} G_{\Delta}(W_{\gamma d}^+) T_{\Delta X}(W_{\gamma d}^+) G_X(W_{\gamma d}^+) \vec{j}_{[2]XN}(\vec{k}) | m \rangle. \quad (14)$$

They are represented in Fig. 3 by the diagrams $\Delta[2]$, $N[2]$, $R\Delta[2]$, and $RN[2]$.

V. RESULTS FOR COHERENT PION PHOTOPRODUCTION

Now we will discuss our results for coherent pion photoproduction on the deuteron. For the explicit calculation we have used a partial wave decomposition. Sufficient convergence is achieved by calculating the contributions NP[1], NP[2], NC[1] and NC[2] of Fig. 4 up to a total angular momentum $j_{max} = 5$, and $\Delta[1]$ up to $j_{max} = 10$. The rescattering graphs R, $\Delta[2]$ and $N[2]$ of Fig. 3 are included up to $j_{max} = 3$.

A. Cross section

We start the discussion with the total cross section plotted in Fig. 6. The dotted curve corresponds to the result of I. Adding MECs ($\Delta[2]$ and $N[2]$) gives a slight increase of a few percent in the maximum (dash-dotted curve). But by far much more important are

the other rescattering mechanisms. They reduce the cross section significantly and shift the maximum to a slightly lower position. Furthermore, a comparison of the full to the dashed curve clearly demonstrates that the perturbative treatment (Born approximation) by replacing

$$T_{\Delta\Delta}(z) \rightarrow V_{\Delta\Delta}^{eff}(z), \quad T_{\Delta N}(z) \rightarrow V_{\Delta N} \quad (15)$$

in the amplitudes of Eqs. (10-11), and (14) is certainly insufficient. It underestimates the full dynamical effect by more than half and thus can provide a qualitative description only.

As shown in Fig. 7 of I, the total cross section is essentially determined by two matrix elements, namely the magnetic dipole $M1(\gamma d) \rightarrow P_2(\pi d)$ and quadrupole $M2(\gamma d) \rightarrow D_3(\pi d)$ transitions. Their importance arises from the coupling to the ${}^5S_2(N\Delta)$ and ${}^5P_3(N\Delta)$ partial waves, respectively. For a more complete list of channel couplings relevant for $\gamma d \rightarrow \pi^0 d$, we refer to Table 1 in I. Unfortunately, the available experimental data for differential cross sections do not allow a reliable determination of total cross sections and thus a check of how well the present model describes the strength of these two leading transitions.

Differential cross sections for fixed pion angles, plotted in Fig. 7, show the same features. For energies in the Δ region, MECs lead to slight increase but further pion rescattering reduces the cross section at all angles. Its influence strongly grows with the pion angle. This qualitatively agrees with what one finds in pion deuteron elastic scattering. Intuitively, one would always expect that rescattering mechanisms become more important at higher momentum transfers, i.e., for larger scattering angles at fixed energy, since rescattering provides the possibility to share the momentum transfer between the two nucleons. In addition, Fig. 7 demonstrates again that the Born approximation gives only a qualitative description of rescattering effects.

As far as the comparison with experimental cross sections is concerned, Fig. 7 shows that the rescattering amplitudes clearly remove most of the discrepancies between the data and our results in I. This conclusion is completely different from the one drawn by Blaazer, Bakker and Boersma [7]. In their work, the three-body rescattering contributions turned out

to be fairly unimportant, namely of the order of a few percent, and could in no way resolve the overestimation of the PWIA cross section. At present we have no explanation for this striking deviation. On the other hand, the rescattering effects of Ref. [9] agree qualitatively with our results. Moreover, the existing differences between these two calculations can essentially be traced back to an insufficient treatment of the charge exchange mechanism in Ref. [9]. This aspect will now be discussed in some detail.

B. The role of charge exchange amplitudes

We have already mentioned that charge exchange amplitudes are dropped within the KMT multiple scattering approach, whereas in our model, the rescattering process includes the exchange of both neutral and charged pions via the successive excitation and decay of the Δ resonance as generated by the driving term in (7). The effect of neglecting the charged pions can directly be determined by splitting the isospin operator occurring in (7) into neutral plus charged pion contributions,

$$\vec{\tau}_{\Delta N}(1) \cdot \vec{\tau}_{N\Delta}(2) = \Omega(\pi^0) + \Omega(\pi^\pm), \quad (16)$$

where

$$\Omega(\pi^0) = \tau_{\Delta N,0}(1) \tau_{N\Delta,0}(2). \quad (17)$$

Now one immediately derives the ratio

$$\frac{\langle \left(\frac{1}{2} \frac{3}{2}\right) 10 | \Omega(\pi_0) | \left(\frac{3}{2} \frac{1}{2}\right) 10 \rangle}{\langle \left(\frac{1}{2} \frac{3}{2}\right) 10 | \Omega(\pi_0) + \Omega(\pi^\pm) | \left(\frac{3}{2} \frac{1}{2}\right) 10 \rangle} = 2, \quad (18)$$

where the coupled two-particle isospin states have been denoted as $|(t_1 t_2) t m_t\rangle$. The ratio (18) implies that the neglect of the exchange of charged pions results in a significant overestimation of the rescattering effect as far as it proceeds through intermediate Δ excitation. In a perturbative treatment it would be just a factor two in the rescattering part of the reaction amplitude.

In order to demonstrate the influence of charge exchange quantitatively, we have performed a calculation for which the charged pion exchange in the driving term $V_{\Delta\Delta}^{eff}(z)$ has been switched off. As a result the differential cross section at 300 MeV is shown in Fig. 8. For a more direct comparison with the results of Kamalov, Tiator and Bennhold, we have collected in Table I relative reduction factors of the differential cross section due to pion rescattering as predicted by the various calculations. Apparently, our calculation without the effect of the exchange of charged pions closely resembles the relative effect of pion rescattering within the KMT formalism. Moreover, the results of Fig. 8 and Table I show that the claim of Ref. [9], namely that contributions from charge exchange becomes small in the Δ resonance region, is not correct.

C. Polarization Observables

In I we have defined all observables corresponding to a polarized photon beam and/or an oriented deuteron target. It turns out that most of the polarization asymmetries are in general less influenced by pion rescattering than the cross section. As a typical example, we show in Fig. 9 the photon asymmetry Σ . Exceptions to this rule are those asymmetries which are not constrained to vanish at 0 and 180 deg, where one observes significant rescattering effects at backward angles. The only single polarization observable of this type, the tensor target asymmetry T_{20} , will now be discussed in greater detail.

1. The tensor target asymmetry T_{20}

For $\gamma d \rightarrow \pi^0 d$ at forward and backward angles, the asymmetry T_{20} allows to draw specific conclusions about details of the reaction mechanism. For this special kinematics, when the pion momentum \vec{q} is parallel or antiparallel to the photon momentum \vec{k} , one has to deal with only two independent reaction amplitudes instead of nine ones in general. This follows from the fact that in the general representation of the full amplitude as $T = \vec{\epsilon}_\lambda \cdot \vec{J}$, the current \vec{J}

has to be constructed from the only available vectors $\hat{k} = \vec{k}/|\vec{k}|$ and \vec{S} , the total deuteron angular momentum. Therefore, one has for the spherical components of \vec{J} at $\theta = 0$ or π

$$J_{\mu}^{[1]} = A(W_{\gamma d}, \theta = 0, \pi) S_{\mu}^{[1]} + \sqrt{10} B(W_{\gamma d}, \theta = 0, \pi) \left[[S^{[1]} \times S^{[1]}]^{[2]} \times [\hat{k}^{[1]} \times \hat{k}^{[1]}]^{[2]} \right]_{\mu}^{[1]}, \quad (19)$$

where the square brackets denote the tensor coupling. The coefficients A and B define the two independent amplitudes. A complete set of the 4 + 5 amplitudes for the general case, where the first ones are constructed in analogy to the four CGLN amplitudes for $\gamma N \rightarrow \pi N$ and the latter five contain the tensor operator $[S^{[1]} \times S^{[1]}]^{[2]}$, will be reported elsewhere [27] together with the expressions for all observables in terms of these amplitudes. In (19), the normalization is chosen such that the cross section is

$$\frac{d\sigma}{d\Omega}(\theta = 0, \pi) \propto |A|^2 + |B|^2. \quad (20)$$

The asymmetry T_{20} then reads

$$T_{20}(\theta = 0, \pi) = -\frac{1}{2\sqrt{2}} \left(1 + 6 \frac{\text{Re}(A^*B)}{|A|^2 + |B|^2} \right). \quad (21)$$

It is restricted to $-\sqrt{2} \leq T_{20} \leq 1/\sqrt{2}$. Obviously, the deviation of T_{20} from $-1/2\sqrt{2}$ is a direct indication of a nonvanishing amplitude B .

It is this amplitude B involving a tensor transition in deuteron spin space which allows to draw some specific conclusions on the reaction mechanism. They are based on the following observations:

(i) In a deuteron model without D wave, \vec{S} is simply given by the sum of the nucleon spins, $\vec{S} = \frac{1}{2} (\vec{\sigma}(1) + \vec{\sigma}(2))$, and thus the tensor operator necessarily involves the spin of both nucleons since $[S^{[1]} \times S^{[1]}]^{[2]} = \frac{1}{2} [\sigma(1) \times \sigma(2)]^{[2]}$. In this case, a nonvanishing B would unambiguously point to a two-nucleon pion production mechanism.

(ii) In a deuteron model with D wave, there are also one-nucleon pion production operators which can contribute to B . However, local one-nucleon operators, i.e., those which are independent from the Fermi momentum of the active nucleon, cannot contribute to B . It is the last statement which makes the situation more conclusive here than for pion deuteron

elastic scattering, where already local one-nucleon scattering operators in combination with the D wave affect T_{20} at extreme angles (see Appendix C).

Thus in general, a nonvanishing B amplitude points to either a two-nucleon or to a nonlocal one-nucleon pion production mechanism, where the latter one has to involve the deuteron D wave. It is not surprising that two-nucleon and D wave effects cannot be separated experimentally since their relative weight is representation dependent. This has been demonstrated explicitly long ago by Friar [28] who showed in a different context that the deuteron quadrupole moment does not allow to fix the deuteron's D wave probability uniquely.

Results for T_{20} are plotted in Fig. 10 for the angles $\theta = 0$ and 180 deg as a function of the photon energy and in Fig. 11 for the photon energies 340 and 400 MeV as a function of the angle θ . The dotted curves include the amplitudes $\Delta[1]$, NP[1] and NC[1] in the notation of Fig. 3 and the disconnected two-body amplitudes (dTBA) NP[2] and NC[2] which have been discussed in I. Particularly at lower energies, they dominate the amplitude B and lead to a significant deviation from $-1/2\sqrt{2}$ as shown by a comparison with the dash-dotted curves where the dTBA have been switched off. MEC contributions $\Delta[2]$ and N[2], added in the dashed curves, show sizeable effects at backward angles and higher energies. Finally, the solid curves include the rescattering term R. In Fig. 10, they introduce a characteristic energy dependence in the Δ region which in principle could be checked experimentally.

In comparison with Ref. [9], one notes a marked disagreement for T_{20} at backward angles. In [9], $T_{20}(\theta = \pi)$ varies only between -0.3 and -0.45 for photon energies between 200 and 400 MeV indicating a much smaller B amplitude. It shows that the (deuteron) spin dependence of the rescattering process is very different in both approaches. On the other hand, this result provides a possibility to distinguish experimentally between both models. With respect to Refs. [7] and [11] we can only compare with results for 300 MeV photon energy where we find good agreement.

We close this subsection with a remark concerning the reaction at threshold. We first note that two nonvanishing amplitudes exist, namely an electric dipole $E1(\gamma d) \rightarrow S_1(\pi d)$ and a

magnetic quadrupole $M2(\gamma d) \rightarrow S_1(\pi d)$. They coincide with A and B , respectively, which become independent of θ at threshold. In view of a test of theoretical predictions for the $\gamma n \rightarrow \pi^0 n$ electric dipole at threshold, e.g., from chiral perturbation theory, a measurement of T_{20} in the near threshold region may be very helpful. Because, according to the above discussion, it could allow to clarify the role of two-nucleon processes which hamper a direct extraction of the neutron amplitude. As a sideremark, we would like to point out that in a very recent study of $\gamma d \rightarrow \pi^0 d$ in the framework of heavy baryon chiral perturbation theory [29] the $M2$ transition has not been considered.

2. The electric quadrupole excitation of the Δ resonance

In I we have studied the sensitivity of the reaction to various elementary pion production multipoles. Within the PWIA the reaction is sensitive to the coherent sum of the $\gamma p \rightarrow \pi^0 p$ and $\gamma n \rightarrow \pi^0 n$ amplitudes, usually denoted as $A^+ = \frac{1}{2}(A^{\pi^0 p} + A^{\pi^0 n})$. Of particular interest is the sensitivity to the E_{1+} multipole which is closely related to the electric quadrupole excitation of the Δ resonance. Already in I, we have pointed out that the vector target asymmetry T_{11} provides an enhanced sensitivity to this quantity. However, before one can draw definite conclusions on the influence of the E_{1+}^+ multipole, the effect of the rescattering contribution has to be investigated.

Our results are summarized in Fig. 12. The unpolarized cross section $d\sigma/d\Omega$ and the cross section difference $\Delta_\sigma = \frac{1}{p_z}(\frac{d\sigma^+}{d\Omega} - \frac{d\sigma^-}{d\Omega})$ rather than the asymmetry T_{11} are plotted for 320 MeV photon energy. Denoting with p_z and p_{zz} the target vector and tensor polarization parameters, respectively, we introduce the cross sections

$$\frac{d\sigma^\pm}{d\Omega} = \frac{d\sigma}{d\Omega} \left[1 \mp \frac{\sqrt{3}}{2} p_z T_{11} - \frac{1}{4} p_{zz} (\sqrt{3} T_{22} + \sqrt{2} T_{20}) \right], \quad (22)$$

with the deuteron orientation axis parallel and antiparallel to $\vec{k} \times \vec{q}$, respectively. In the unpolarized cross section, the rescattering strongly masks the E2 excitation of the Δ . On the contrary, in the difference Δ_σ the rescattering effect is suppressed whereas the E2 leads

to a change of the order of 50% in the most promising region between $\theta = 20$ and 30 deg. Assuming $p_z \approx 1$, $p_{zz} \approx 0$, the cross sections actually to be measured are of the order $d\sigma^+/d\Omega \approx 15 \mu b/sr$ and $d\sigma^-/d\Omega \approx 45 \mu b/sr$.

VI. SUMMARY AND CONCLUSION

In this paper we have studied the influence of pion rescattering on coherent pion photoproduction off the deuteron in the Δ resonance region. The calculation is based on a dynamical model which includes the coupling of $N\Delta$, $NN\pi$ and NN channels. Our main conclusions are as follows. Pion rescattering is significant and reduces the cross section in the resonance region. The strongest influence appears at large momentum transfers (backward pion angles). This means in particular with respect to a test of theoretical models for pion production amplitudes on the neutron that one needs a reliable description for the rescattering process. Compared to experimental data, we find that the sizeable discrepancies without rescattering as reported in I, are largely reduced and that a reasonable agreement with the data is achieved.

Furthermore, we have shown that a perturbative treatment of rescattering, which is comparable to a double-scattering ansatz, can only give a qualitative description of rescattering effects. The inclusion of charged pion exchange, i.e., the coupling to the intermediate π^+nn and π^-pp break-up channels is by no means unimportant as was claimed in [9]. Its neglect leads to a sizeable overestimation of the rescattering effect. This observation could essentially explain the differences with respect to the relative strength of the rescattering process between this work and the results of Ref. [9] which are based on the KMT multiple scattering approach. However, the discrepancies to the results of Ref. [7] using a Faddeev ansatz remain unclear.

Most of the polarization observables are less sensitive to rescattering than the cross section. As an exception, we have stressed the role of the tensor target asymmetry T_{20} as a tool to disentangle different reaction mechanisms. Particularly, its measurement at backward

pion angles would be very helpful. Incidentally, it would allow to distinguish between the present model and the one of Ref. [9]. In Ref. [1], we have already pointed out a remarkable sensitivity of the vector target asymmetry T_{11} on the E2 excitation of the Δ resonance. Our analysis here shows that rescattering effects do not seriously mask this sensitivity. In the most favorable case, such effects are suppressed by about a factor 5 compared to the E2 effect.

APPENDIX: A

Using a partial wave decomposition, Eq. (3) reduces to a one-dimensional integral equation which has to be solved numerically. Its solution is hampered by the presence of logarithmic three-body singularities which occur in $V_{\Delta\Delta}^{ret}(E^+)$ as a consequence of the coupling to the open πNN channel. In order to overcome this problem, we have iterated the integral equation once. Introducing for the moment being a more convenient and obvious matrix notation we can write (3) in the form

$$\mathcal{T} = \mathcal{V} + \mathcal{V}\mathcal{G}\mathcal{T}. \quad (\text{A1})$$

The once iterated equation $\mathcal{T} = \mathcal{V} + \mathcal{V}\mathcal{G}\mathcal{V} + \mathcal{V}\mathcal{G}\mathcal{V}\mathcal{G}\mathcal{T}$ can be rewritten as an integral equation for the difference $\mathcal{T} - \mathcal{V}$,

$$\mathcal{T} - \mathcal{V} = \mathcal{V}\mathcal{G}\mathcal{V} + \mathcal{V}\mathcal{G}\mathcal{V}\mathcal{G}\mathcal{V} + \mathcal{V}\mathcal{G}\mathcal{V}\mathcal{G}(\mathcal{T} - \mathcal{V}). \quad (\text{A2})$$

The advantage of (A2) is that both, the kernel $\mathcal{V}\mathcal{G}\mathcal{V}\mathcal{G}$ as well as the inhomogeneous term $\mathcal{V}\mathcal{G}\mathcal{V} + \mathcal{V}\mathcal{G}\mathcal{V}\mathcal{G}\mathcal{V}$, are smooth quantities since the three-body singularities contained in \mathcal{V} have been integrated over. Thus it can be solved numerically by applying the matrix inversion technique after a discretization in momentum space.

APPENDIX: B

The two-body current $\vec{j}_{[2]\Delta N}^\pi$ has to be constructed consistent to the π exchange in the transition potential which reads

$$V_{N\Delta}^\pi = -\frac{f_{\pi NN}f_{\pi N\Delta}}{m_\pi^2}\vec{\tau}_{NN}(1)\cdot\vec{\tau}_{N\Delta}(2) \quad (\text{B1})$$

$$\int \frac{d^3q}{(2\pi)^3} e^{i\vec{q}\cdot\vec{r}} \frac{\vec{\sigma}_{NN}(1)\cdot\vec{q}\vec{\sigma}_{N\Delta}(2)\cdot\vec{q}}{\vec{q}^2+m_\pi^2} F_{\pi NN}(\vec{q}^2)F_{\pi N\Delta}(\vec{q}^2) + (1\leftrightarrow 2),$$

where \vec{r} is the relative coordinate of the two baryons. In the present version of our model (without ρ exchange in $V_{N\Delta}$), the form factors have been taken in monopole form

$$F_{\pi N\Delta}(\vec{q}^2) = F_{\pi NN}(\vec{q}^2) = \frac{\Lambda_\pi^2 - m_\pi^2}{\Lambda_\pi^2 + \vec{q}^2}, \quad (\text{B2})$$

where $\Lambda_\pi = 700$ MeV has been determined by fitting the NN scattering data in the 1D_2 channel (see [19]) using $f_{\pi NN}^2/4\pi = 0.08$ and $f_{\pi N\Delta}^2/4\pi = 0.35$. The MEC can be written as

$$\vec{j}_{[2]\Delta N}^\pi(\vec{k}) = ie(\vec{\tau}_{\Delta N}(1)\times\vec{\tau}_{NN}(2))_0 \frac{f_{\pi N\Delta}f_{\pi NN}}{m_\pi^2} \int \frac{d^3q}{(2\pi)^3} e^{i\vec{q}\cdot\vec{r}} \sum_{x=k_\pm,\pi,v} \vec{V}^x\Gamma^x + (1\leftrightarrow 2), \quad (\text{B3})$$

where the vertex and propagator structures of the contact (k_\pm), pion-in-flight (π), and vertex regularization (v) currents are given by

$$\vec{V}^{k_-} = \vec{\sigma}_{\Delta N}(1)\vec{\sigma}_{NN}(2)\cdot(\vec{q}-\vec{k}/2), \quad (\text{B4})$$

$$\vec{V}^{k_+} = \vec{\sigma}_{NN}(2)\vec{\sigma}_{\Delta N}(1)\cdot(\vec{q}+\vec{k}/2), \quad (\text{B5})$$

$$\vec{V}^\pi = \vec{V}^v = \vec{q}\vec{\sigma}_{\Delta N}(1)\cdot(\vec{q}+\vec{k}/2)\vec{\sigma}_{NN}(2)\cdot(\vec{q}-\vec{k}/2), \quad (\text{B6})$$

$$\Gamma^{k_\pm} = \frac{F_{\pi N\Delta\pm}F_{\pi NN\pm}}{\omega_\pm^2}, \quad (\text{B7})$$

$$\Gamma^\pi = -2\frac{F_{\pi N\Delta+}F_{\pi NN-}}{\omega_+\omega_-^2}, \quad (\text{B8})$$

$$\Gamma^v = 2\frac{F_{\pi N\Delta+}-F_{\pi N\Delta-}}{\omega_+^2-\omega_-^2}\frac{F_{\pi NN-}}{\omega_-^2} + 2\frac{F_{\pi NN+}-F_{\pi NN-}}{\omega_+^2-\omega_-^2}\frac{F_{\pi N\Delta+}}{\omega_+^2}, \quad (\text{B9})$$

with $\omega^2 = \vec{q}^2 + m_\pi^2$ and using the notation $f_\pm = f(\vec{q}\pm\vec{k}/2)$ for any function $f(\vec{q})$. The two-nucleon currents $\vec{j}_{[2]NN}^\pi$ and $\vec{j}_{[2]NN}^\rho$ consistent to the OBEPR potential may be found in [30].

APPENDIX: C

First we show that local one-nucleon operators cannot contribute to the tensor transition amplitude B defined in (19). In general, all transitions which contribute to a coherent

deuteron reaction can be classified as scalar, vector, and tensor (rank 2) transitions with respect to the deuteron angular momentum space. In order to identify them for a given transition operator \mathcal{O} , we start by writing the deuteron wave function with magnetic quantum number m as

$$\psi_m(\vec{r}) = \frac{1}{\sqrt{4\pi}} \frac{1}{r} \left(u_0(r) + \frac{1}{\sqrt{8}} S_{12} u_2(r) \right) \left| \left(\frac{1}{2} \frac{1}{2} \right) 1m \right\rangle, \quad (\text{C1})$$

where $S_{12} = 3\vec{\sigma}(1) \cdot \hat{r} \vec{\sigma}(2) \cdot \hat{r} - \vec{\sigma}(1) \cdot \vec{\sigma}(2)$. For a $S \leftrightarrow S$, $S \leftrightarrow D$, or $D \leftrightarrow D$ transition one has to consider with respect to the spin degrees of freedom the effective operators

$$\mathcal{O}_{SS} = \mathcal{O}, \quad (\text{C2})$$

$$\mathcal{O}_{SD} = S_{12}\mathcal{O} + \mathcal{O}S_{12}, \quad (\text{C3})$$

$$\mathcal{O}_{DD} = S_{12}\mathcal{O}S_{12}, \quad (\text{C4})$$

respectively. Note, that \mathcal{O} itself may depend on $\vec{\sigma}(1)$ and $\vec{\sigma}(2)$. Using the following equivalences valid within the space $\left\{ \left| \left(\frac{1}{2} \frac{1}{2} \right) 1m \right\rangle \right\}$

$$\vec{\sigma}(1) \cdot \vec{\sigma}(2) \simeq 1, \quad (\text{C5})$$

$$\vec{\sigma}(1) + \vec{\sigma}(2) \simeq 2\vec{S}, \quad (\text{C6})$$

$$\vec{\sigma}(1) - \vec{\sigma}(2) \simeq 0, \quad (\text{C7})$$

$$\vec{\sigma}(1) \times \vec{\sigma}(2) \simeq 0, \quad (\text{C8})$$

$$\left[\sigma^{[1]}(1) \times \sigma^{[1]}(2) \right]^{[2]} \simeq 2S^{[2]}, \quad (\text{C9})$$

$$(\text{C10})$$

where \vec{S} is the total deuteron angular momentum and $S^{[2]} = \left[S^{[1]} \times S^{[1]} \right]^{[2]}$, one can rewrite the effective operators \mathcal{O}_T ($T = SS, SD, DD$) as

$$\mathcal{O}_T = \mathcal{O}_T^{[0]} + \left[\mathcal{O}_T^{[1]} \times S^{[1]} \right]^{[0]} + \left[\mathcal{O}_T^{[2]} \times S^{[2]} \right]^{[0]}, \quad (\text{C11})$$

where $\mathcal{O}_T^{[L]}$ does not contain any spin operators.

In our case, namely for $\gamma d \rightarrow \pi^0 d$ at 0 or 180 deg, any local one-nucleon operator has the structure $\vec{\sigma} \cdot \vec{v}$ with a vector \vec{v} and $[\vec{v}, \vec{r}] = 0$, since no local pseudovector apart from $\vec{\sigma}$ is

available (a nonlocal one would be given by $\vec{p} \times \hat{k}$ where \vec{p} is the nucleon momentum). The above statement then follows using the identities

$$S_{12} \vec{\sigma}(1/2) \cdot \vec{v} + \vec{\sigma}(1/2) \cdot \vec{v} S_{12} = 6\vec{v} \cdot \hat{r} \vec{\sigma}(2/1) \cdot \hat{r} - 2\vec{\sigma}(2/1) \cdot \vec{v}, \quad (\text{C12})$$

$$S_{12} \vec{\sigma}(1/2) \cdot \vec{v} S_{12} = (\vec{\sigma}(1) + \vec{\sigma}(2)) \cdot (6\vec{v} \cdot \hat{r} \hat{r} - 4\vec{v}), \quad (\text{C13})$$

which do not contain a tensor transition on their right hand sides.

Next, we point out the difference of $\gamma d \rightarrow \pi^0 d$ to the case of the $\pi d \rightarrow \pi d$ reaction at 0 or 180 deg. For the latter reaction, the analogous relation of Eq. (19) reads

$$T_{\pi d} = A(W_{\pi d}, \theta = 0, \pi) + \frac{3}{2} \sqrt{10} B(W_{\pi d}, \theta = 0, \pi) \left[S^{[2]} \times \left[\hat{k}^{[1]} \times \hat{k}^{[1]} \right]^{[2]} \right]_0^{[0]}, \quad (\text{C14})$$

with corresponding cross section as in (20). The asymmetry is given by

$$T_{20}(\theta = 0, \pi) = -\frac{1}{\sqrt{2}} \frac{|B|^2 - 2\sqrt{2} \text{Re}(A^* B)}{|A|^2 + |B|^2}. \quad (\text{C15})$$

In the case of pion scattering, one deals with scalar transition operators and thus already local one-nucleon operators involving $S \leftrightarrow D$ or $D \leftrightarrow D$ transitions contribute to the amplitude B which can be observed by means of the deviation from $T_{20} = 0$ at extreme angles.

REFERENCES

- [1] P. Wilhelm and H. Arenhövel, Nucl. Phys. A 593 (1995) 435.
- [2] F. Blaazer, B.L.G. Bakker and H.J. Boersma, Nucl. Phys. A 568 (1994) 681.
- [3] P. Osland and A.K. Rej, Nuovo Cimento 32A (1976) 469.
- [4] C. Lazard, R.J. Lombard and Z. Maric, Nucl. Phys. A 271 (1976) 317.
- [5] P. Bosted and J.M. Laget, Nucl. Phys. A 296 (1978) 413.
- [6] H. Garcilazo and E. Moya de Guerra, Phys. Rev. C 49 (1995) 49.
- [7] F. Blaazer, B.L.G. Bakker and H.J. Boersma, Nucl. Phys. A 590 (1995) 750.
- [8] A.K. Kerman, H. Mc Manus and R.M. Thaler, Ann. Phys. 8 (1959) 551.
- [9] S.S. Kamalov, L. Tiator and C. Bennhold, Mainz preprint MKPH-T-95-22.
- [10] S.S. Kamalov, L. Tiator and C. Bennhold, Mainz preprint MKPH-T-95-21.
- [11] M.T. Peña, H. Garcilazo, U. Oelfke and P.U. Sauer, Phys. Rev. C 45 (1992) 1487.
- [12] P.U. Sauer, Prog. Part. Nucl. Phys. 16 (1986) 35.
- [13] H. Pöpping, P.U. Sauer and X.-Z. Zhang, Nucl. Phys. A474 (1987) 557.
- [14] M. Betz and T.-S.H. Lee, Phys. Rev. C 23 (1981) 375.
- [15] T.-S.H. Lee, Phys. Rev. Lett. 50 (1983) 1571.
- [16] T.-S.H. Lee, Phys. Rev. C 29 (1984) 195.
- [17] T.-S.H. Lee and A. Matsuyama, Phys. Rev. C 32 (1985) 1986; Phys. Rev. C 36 (1987) 1459.
- [18] R. Machleidt, K. Holinde, and Ch. Elster, Phys. Reports 149 (1987) 1.
- [19] P. Wilhelm and H. Arenhövel, Phys. Lett. B 318 (1993) 410.

- [20] K. Gabathuler et al., Nucl. Phys. A 350 (1980) 253.
- [21] C.R. Ottermann et al., Phys. Rev. C 32 (1985) 928.
- [22] E. Hilger et al., Nucl. Phys. B 93 (1975) 7.
- [23] G. von Holtey et al., Z. Phys. 259 (1973) 51.
- [24] B. Bouquet et al., Nucl. Phys. B 79 (1974) 45.
- [25] K. Baba et al., Phys. Rev. C 28 (1983) 286.
- [26] W. Beulertz, Ph.D. thesis, Universität Bonn, 1994.
- [27] P. Wilhelm and H. Arenhövel, to be published.
- [28] J.L. Friar, Phys. Rev. C 20 (1979) 325.
- [29] S.R. Beane, C.Y. Lee, and U. van Kolck, Phys. Rev. C 52 (1995) 2914.
- [30] K.-M. Schmitt and H. Arenhövel, Few-Body Syst. 7 (1989) 95.

FIGURES

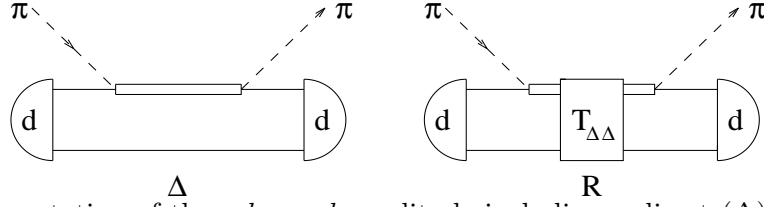


FIG. 1. Representation of the $\pi d \rightarrow \pi d$ amplitude including a direct (Δ) and a rescattering amplitude (R).

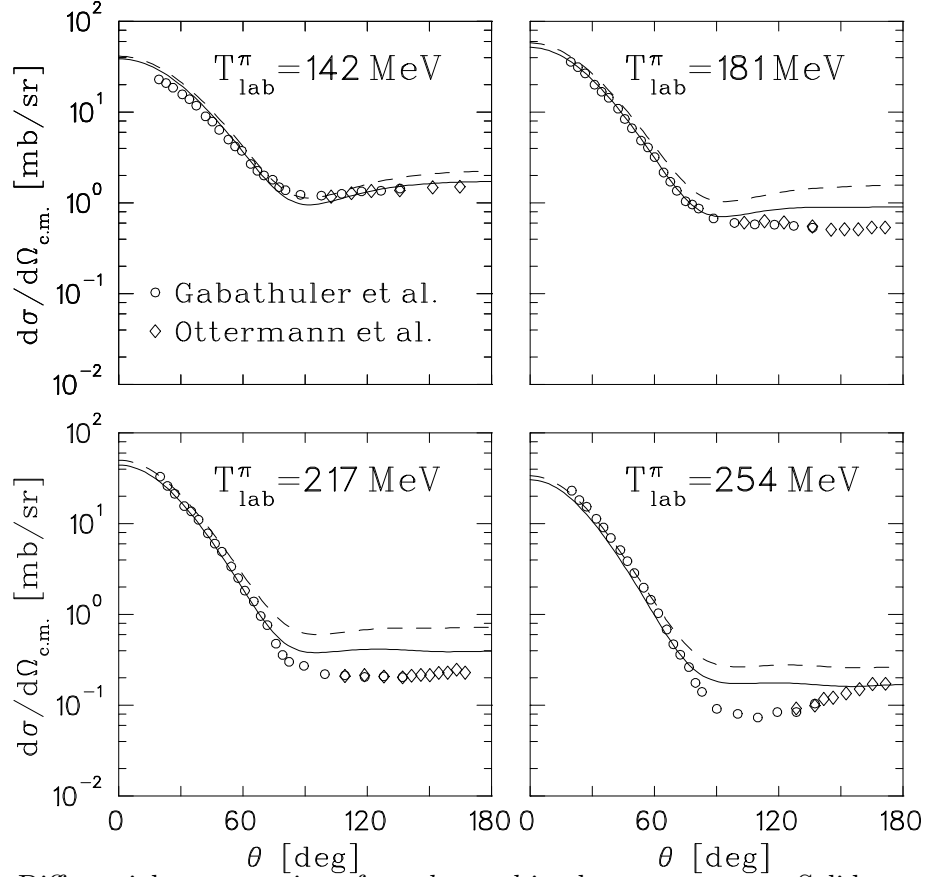


FIG. 2. Differential cross sections for $\pi d \rightarrow \pi d$ in the c.m. system. Solid curves: complete calculation, and dashed curves: without rescattering (R). Experimental data from [20] (circles) and [21] (rhombs).

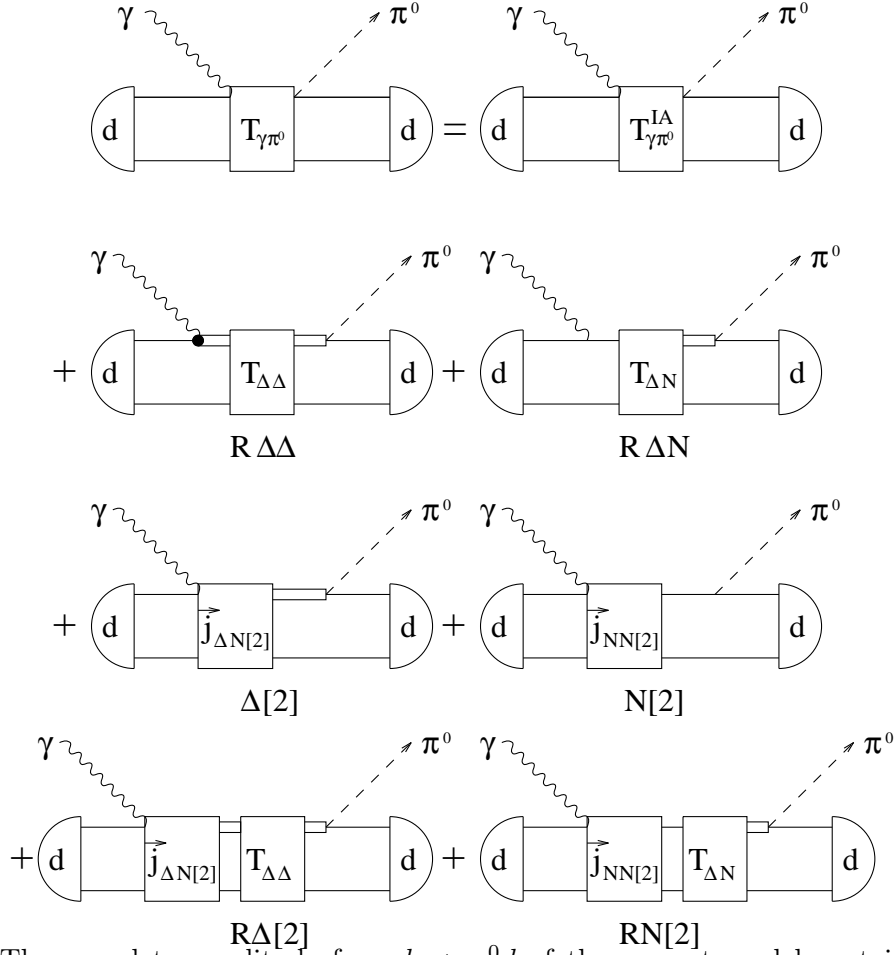


FIG. 3. The complete amplitude for $\gamma d \rightarrow \pi^0 d$ of the present model contains the direct contributions $T_{\gamma\pi^0}^{IA}$ defined in I and shown in Fig. 4 and rescattering contributions. The latter are the graphs generated by the hadronic T -matrices $R\Delta\Delta$ and $R\Delta N$, the MEC graphs $\Delta[2]$ and $N[2]$, and the graphs which combine MECs and T -matrices $R\Delta[2]$ and $RN[2]$. The short-hand notation $R=\{R\Delta\Delta, R\Delta N, R\Delta[2], RN[2]\}$ is used in the text.

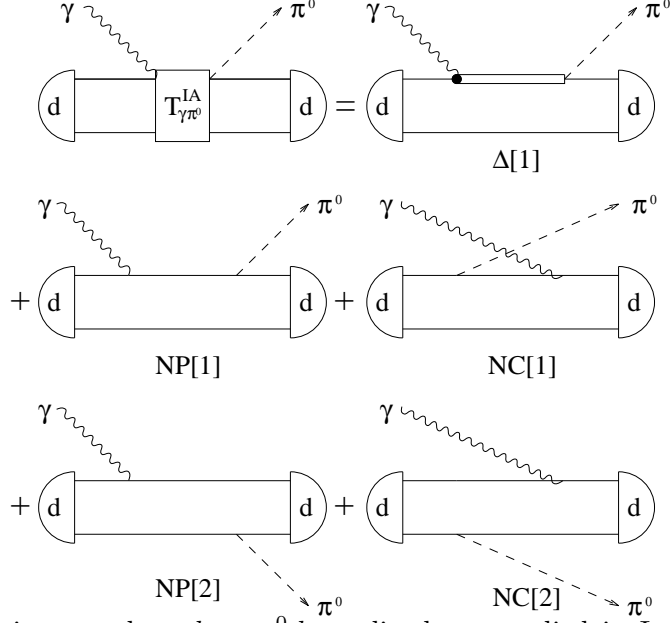


FIG. 4. Contributions to the $\gamma d \rightarrow \pi^0 d$ amplitude as studied in I: direct Δ contribution $\Delta[1]$, direct NP[1] and crossed NC[1] nucleon pole, direct NP[2] and crossed NC[2] disconnected two-body processes.

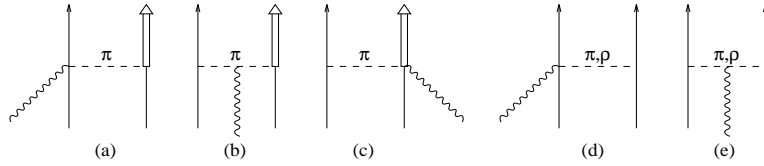


FIG. 5. MEC contributions included in the present calculation. $\vec{J}_{[2]\Delta N}^{\pi}$: (a)–(c), and $\vec{J}_{[2]NN}^{\pi(\rho)}$: (d) and (e).

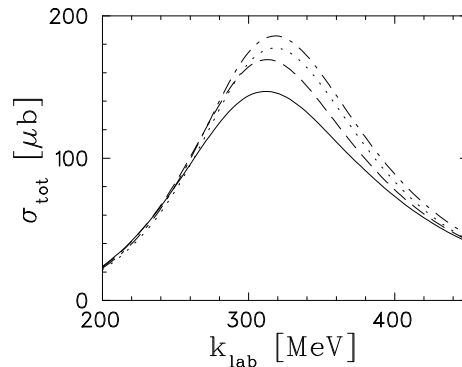


FIG. 6. Total cross section for $\gamma d \rightarrow \pi^0 d$. Solid curve: complete calculation, dotted curve: without rescattering amplitudes (R, $\Delta[2]$, N[2]), dash-dotted curve: without R, and dashed curve: Born approximation according to Eq. (15).

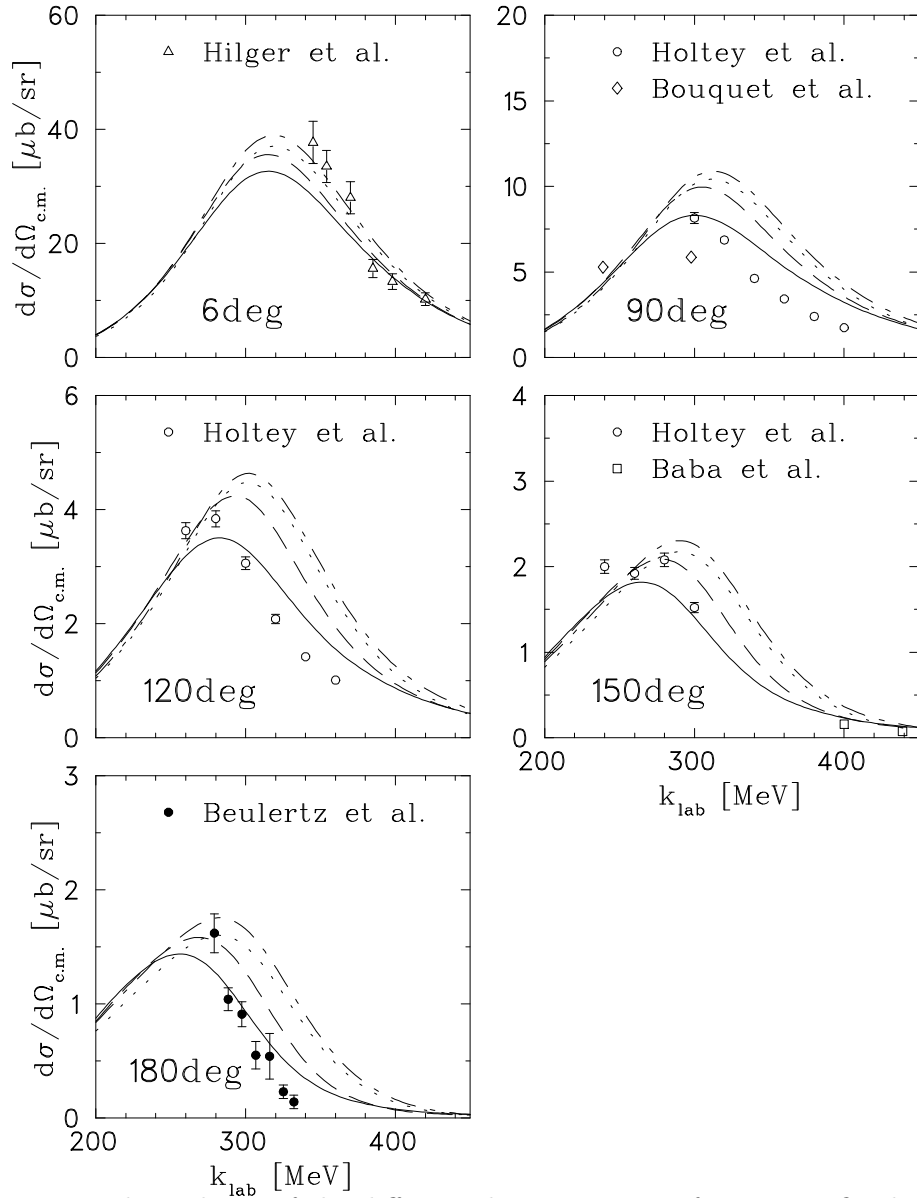


FIG. 7. Energy dependence of the differential cross sections for various fixed pion angles θ .

Notation as in Fig. 6. Experimental data from [22–26].

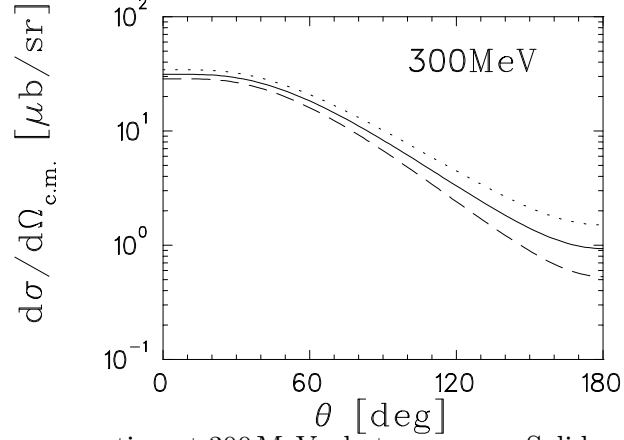


FIG. 8. Differential cross section at 300 MeV photon energy. Solid and dotted curves are as in Fig. 6. Dashed curve: complete calculation without charged pion exchange in $V_{\Delta\Delta}^{eff}(z)$ as explained in the text.

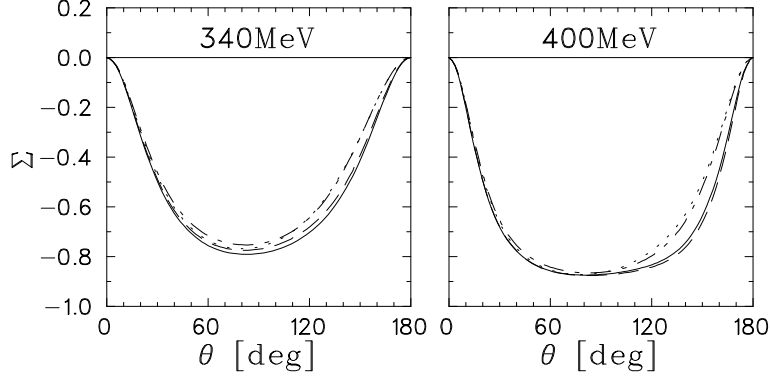


FIG. 9. Photon asymmetry Σ at 340 and 400 MeV photon energy. Notation as in Fig. 6.

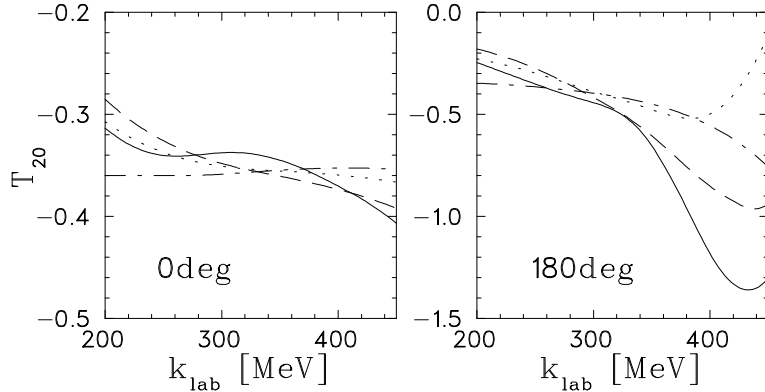


FIG. 10. Energy dependence of the tensor target asymmetry T_{20} at 0 and 180 deg. Dash-dotted curves include $\Delta[1]$, NP[1], NC[1] and then consecutively added dTBA contribution NP[2], NC[2] (dotted), MEC contribution $\Delta[2]$, N[2] (dashed), and further rescattering R (solid).

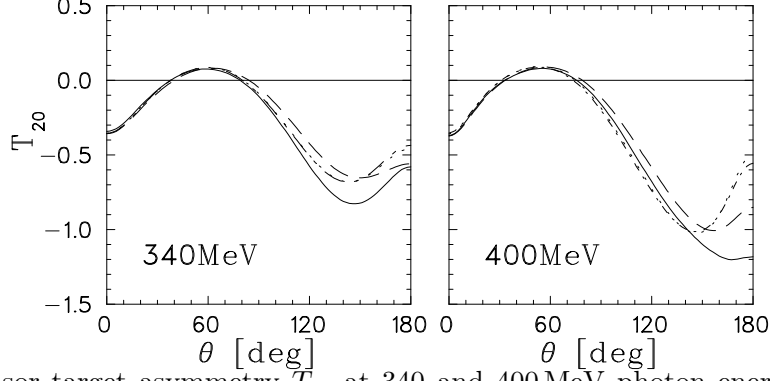


FIG. 11. Tensor target asymmetry T_{20} at 340 and 400 MeV photon energy. Notation as in Fig. 10.

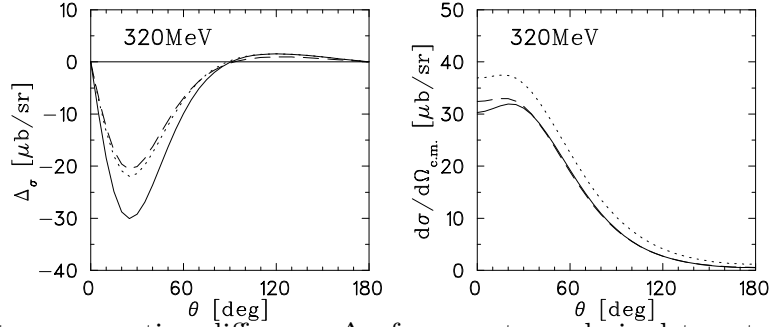


FIG. 12. Left: cross section difference Δ_σ for a vector polarized target, right: unpolarized cross section $d\sigma/d\Omega$ at 320 MeV photon energy. Solid curve: complete calculation with inclusion of the E2 excitation of the Δ , dashed curve: without E2 contribution, and dotted curve: without rescattering contributions (R, $\Delta[2]$, N[2]) and without E2.

TABLES

TABLE I. Relative reduction factors of the differential cross section at 300 MeV photon energy for various pion angles due to pion rescattering. The second and third column correspond to the ratios of the dotted to the solid and to the dashed curves in Fig. 8, respectively. The last column contains the ratios as read off from the dashed and solid curves in Fig. 4 of Ref. [9].

θ (deg)	this model with π^\pm	this model without π^\pm	model of Ref. [9]
0	1.10	1.20	1.3
90	1.22	1.51	1.5
180	1.61	2.83	3.0